

10. Ando, W. and Tsumaki, H., *Synth. Commun.*, 1983, **13**, 1053–1056.
11. Taylor, E. C. Mclay, G. W. and McKillop, A., *J. Am. Chem. Soc.*, 1968, **90**, 2422–2423.
12. Illi, V. O., *Tetrahedron Lett.*, 1979, **20**, 2431–2432.
13. Chowrasia, D. and Sharma, N., Solvent substitution evaluation of limestone water as a medium for benzooylation. *Arch. Chem. Res.*, 2016, **1**, 1.
14. Paul, S., Nanda, P. and Gupta, R., PhCOCl–Py/basic alumina as a versatile reagent for benzooylation in solvent-free conditions. *Molecules*, 2003, **8**, 374–380.
15. Murray, R. K., Granner, D. K., Mayer, P. A. and Rodwell, V. W., Structure and function of water-soluble vitamins. In *Harper's Biochemistry*, Appleton & Lange, Stamford, 1996, vol. 24, pp. 599–600.
16. Bernhard, S., *The Structure and Function of Enzymes*, W. A. Benjamin, New York, USA, 1968, Chap. 7.
17. Bruice, T. C. and Benkovic, S., *Bioorganic Mechanism*, W. A. Benjamin, New York, USA, 1966, vol. 2.
18. Lowe, J. N. and Ingraham, L. L., *An Introduction to Biochemical Reaction Mechanisms*, Englewood Cliffs, Prentice-Hall, NJ, USA, 1974, Chap. 5.
19. Eicher, T., Hauptmann, S. and Speicher, A., Five membered heterocycles. In *The Chemistry of Heterocycles-Structure, Reaction, Synthesis, and Applications*, Wiley-VCH GmbH & Co. KGaA, Weinheim, 2003, 2nd edn, pp. 154–155.
20. Lobell, M. and Grout, D. H. G., *J. Am. Chem. Soc.*, 1996, **118**, 1867.
21. Stetter, H. and Dämbkes, G., *Synthesis*, 1977, **6**, 403.
22. <http://www.umsl.edu/~orglab/pdffiles/multistp.pdf>
23. <http://www.stpaulschool.org.uk/resource.aspx?id=136714>

Received 18 January 2018; accepted 21 May 2018

doi: 10.18520/cs/v115/i11/2130-2133

Degraded products of stem bromelain destabilize aggregates of β -amyloid peptides involved in Alzheimer's disease

Debratna Mukherjee¹, Payel Bhattacharjee¹,
Reema Bhattacharya¹, Alok K. Dutta¹ and
Debasish Bhattacharyya^{1,2,*}

¹Division of Structural Biology and Bioinformatics, CSIR-Indian Institute of Chemical Biology 4, Raja S.C. Mallick Road, Jadavpur, Kolkata 700 032, India

²Department of Zoology, Tripura University, Surjyamani Nagar, Bikramnagar 799 022, India

Deposition of fibrils originating from monomeric β -amyloid ($A\beta$) peptide in brain cells is responsible for progressive neuronal damages in Alzheimer's disease. Peptides from bromelain, a cysteine protease from *Ananas comosus* (pineapple), were generated after digestion with proteases under conditions similar to human gastrointestinal tract. These peptides not only

inhibit the growth of $A\beta$ -amyloid aggregates, but also irreversibly destabilize the preformed aggregates. Gel filtration followed by mass spectrometric analysis identified a pool of peptides of <700 Da in the digest. Probable composition of the peptides interacting with $A\beta$ -peptide was predicted from homology alignment between $A\beta$ -peptide and bromelain using bioinformatics tools. Corresponding synthetic peptides can also destabilize the preformed aggregates as observed from thioflavin T assay, transmission electron microscopy and atomic force microscopy. $A\beta$ aggregates that were preincubated with the bromelain-derived peptides did not exert appreciable toxicity on human neuroblastoma cells (SH-SY5Y) cultured *in vitro*.

Keywords: Alzheimer's disease, $A\beta$ peptide, disaggregation, stem bromelain.

PROTEIN aggregation is one of the consequences of cellular events. Their accumulation is related to neuronal degeneration and organ failure¹. Alzheimer's disease (AD) is an irreversible degeneration of the brain that causes dementia followed by cognition impairment and loss of memory. The impairment of cognition in human brain is caused by deposition of the aggregates of β -amyloid ($A\beta$) peptide in a progressive manner since the initiation of the process². Even the soluble oligomers of $A\beta$ peptide are cytotoxic to neuronal cells. It is unclear how the equilibration between the free, nonpathogenic monomeric peptides and the oligomers that are forerunners of the aggregate is disturbed³. As of today, no natural product or synthetic compound has been discovered as a drug to prevent or cure AD.

Pineapple (*Ananas comosus*) is a medicinal plant. All parts of the plant contain high level of protease activity. The plant extracts are collectively known as bromelain. Medicinal properties of bromelain are brought about synergistically by an array of enzymes present in it⁴. Stem bromelain, the major cysteine protease of the extract from pineapple stem, is commercially available⁵. Bromelain has broad specificity towards hydrolysis of peptide bonds and offers a wide range of therapeutic activities^{6–9}. Due to its efficiency after oral administration, safety and lack of undesired side effects, bromelain is being increasingly considered as a phyto-therapeutic drug^{7,10}.

In recent years, the role of proteases in the pathogenesis, diagnosis and treatment of amyloid peptide-related diseases has been extensively studied^{11,12}. Generally, amyloid fibrils are stable, rich in β -sheet content and are resistant to proteases¹³. However, this notion is not universally valid. Cathepsin B, a lysosomal cysteine protease, plays a crucial role in intracellular proteolysis. Upregulation of this enzyme is observed in a number of clinical conditions. Anti-amiloidogenic and related neuroprotective function of cathepsin B against $A\beta$ peptides has been reported¹⁴. Subsequently, cystatin C, a cysteine protease inhibitor that inactivates cathepsin B, has further confirmed

*For correspondence. (e-mail: dbhattacharyya1957@gmail.com)

the role of the latter in regulating the formation of A β aggregate. In humans, all cells containing nucleus produce cystatin C and it is available essentially in all body fluids and tissues. Formation of cathepsin B–cystatin C conjugate causes upregulation of A β aggregate and AD¹⁵. Currently, the regulatory roles of proteases in the biosynthetic pathway of A β peptide and formation of corresponding aggregate from the monomeric peptide are well established¹⁶. With further advancement of information, the role of this class of cysteine proteases in AD has been fairly confirmed¹⁷.

During studies on stem bromelain, we observed that it can destabilize A β -aggregate¹⁸. It may originate from direct proteolysis of the aggregate. Alternately, a pool of peptides that are generated arising from 'auto-digestion' of bromelain may be the causative agent. These peptides may act as potent molecules to interact with the aggregates leading to their disintegration to near-monomeric state. To distinguish this, inactive bromelain devoid of proteolytic activity was prepared. This nonfunctional molecule can also destabilize the aggregates. Therefore, the role of amino acid stretches of bromelain in the process of destabilization is suggestive¹⁸. Of course, this does not exclude proteolysis of amyloid aggregates by bromelain itself. Here, we present that small peptides generated from bromelain after protease digestion as per human digestive system show potent destabilization of A β -aggregates. Small synthetic peptides, the sequences of which have been derived from the template of bromelain, also show destabilization of A β -aggregates.

Fine chemicals were procured as follows: carboxypeptidase (bovine pancreas), α -chymotrypsin (bovine pancreas), elastase (porcine pancreas), Sephadex G-50 and G-10, stem bromelain (E.C. 3.4.22.32, lyophilized powder containing 60% of protein), trypsin (bovine pancreas, grade I) from Sigma, USA; 1,1,1,3,3,3-hexafluoro-2-propanol (HFIP) from Sigma-Aldrich, St Louis, USA; pepsin and dimethyl sulphoxide (DMSO) from SRL, Mumbai, India; Dulbecco's modified eagle medium (DMEM), Ham's modification of F-12, phosphate buffered saline (PBS), heat-inactivated fetal bovine serum (FBS), 3-[4,5-dimethylthiazol-2-yl]-2,5-diphenyltetrazolium bromide (MTT), L-glutamine, penicillin/streptomycin, gentamycin, fungizone and trypsin solution from GibcoTM, Invitrogen, Paisley, UK and A β 40 and A β 42 peptides (>95% purity) from American Peptide Company, USA. Synthetic peptides KKW (461.28 Da, 174–176 position in bromelain), KWGA (175–178), WGAK (176–179), GAKW (177–180), AKWG (178–181, 461.28 Da each) and NPCGACWA (821.31 Da, 21–28) were from GenPro Biotech, New Delhi, India. Purity of the synthetic peptides was demonstrated by RP-HPLC and mass analysis. Brush border membrane (BBM) proteases were extracted from the intestine of freshly slaughtered goat¹⁹.

Protein components of commercially available stem bromelain were separated using size-exclusion chromato-

graphy¹⁸. Stem bromelain (10 mg/ml) was suspended in 10 mM Na-phosphate, pH 7.5 (buffer A) at 4°C for 16 h. After centrifugation at 8000 g for 15 min, 2.5 ml of the supernatant was applied onto a Sephadex G-50 column (1.5 × 90 cm) equilibrated with buffer A. The chromatogram separated the components into two fractions. Protease activity that was confined to the first fraction was pooled. The second fraction contained the pigments, small peptides and unidentified small molecules. The protein fraction showed single band in 10% PAGE at pH 7.5 and zymography using bovine serum albumin as substrate²⁰. Proteolytic activity was measured using azocasein as substrate²¹.

Formation of β -amyloid peptide of amino acid length 40/42 (A β 40/42) aggregates from the monomeric states of the peptides was standardized in the laboratory. The peptide (3 mg) was dissolved in 1 ml of 1,1,1,3,3,3-hexafluoro-2-propanol (HFIP) and sonicated (Roop-Telsonic, Ultrasonix Ltd, UK, Tec-25, compact ultrasonic cleaner) for 15 min at 4°C. Then it was passed through Millex-FG 0.22 μ m filter membrane (Millipore, USA) to remove traces of insoluble seeds or preformed aggregates. The solution was kept at 25°C for 16 h to form a homogeneous solution. It was followed by complete evaporation of the solvent. The dried layer was dissolved in DMSO to prepare a stock solution of 3.46 mM of the peptide. To prepare a working solution of 10 μ M, dilution was done in one step from the stock solution into buffer A containing 100 mM NaCl. The working solution was incubated at 37°C with stirring for 16 h to prepare soluble aggregates of A β .

In the fluorimetric estimation of aggregate formation, thioflavin T (ThT) assay was performed. ThT (10 μ l, 250 μ M in water, $\epsilon_{412\text{ nm}} = 35,000\text{ M}^{-1}\text{ cm}^{-1}$, ex: 450 nm; em: 480–600 nm) was added to A β 40/42 aggregate (10 μ M) and the volume was made up to 1 ml by buffer A containing 100 mM NaCl²². To follow the time course of disaggregation, A β 40/42 aggregates (10 μ M) were incubated in presence of 0.01–10 μ M of bromelain-derived peptides at 37°C for 15 days. Aliquots were withdrawn at an interval of 3 days and disaggregation was followed from ThT assay. Bromelain-derived peptide solution in the absence of A β aggregates was also incubated under identical conditions. This served as control to follow self-aggregation of these peptides. A Hitachi F-4500 spectrofluorimeter (slit width 10/10 nm) attached with a circulating water bath was used.

For transmission electron microscope (TEM) images, test sample (10 μ l) was placed on a carbon-coated 300-mesh copper grid (GSCu300C, ProSciTech, Australia) for 1 min at 25°C and the unbound substrates were removed using blotting paper. To stain the adhered particles, the grid was treated with 2% uranyl acetate for 20 s and excess reagent was removed as mentioned earlier. The grid was dried for 15 min and analysed with a TEM (model FEI TECNAI G2 Spirit BioTwin, Czech Republic)

operating at an accelerating voltage of 80 kV (115,000 ×). For atomic force microscopy (AFM) images, test sample (10 μl) was placed on freshly cleaved pyrolytic graphite (HOPG) surface for 20 min and thereafter dried under vacuum. Sometimes the sample was gently washed with deionized Milli-Q water to remove unattached molecules. Acoustic AC-mode AFM was used with a Pico plus 5500 AFM (Agilent Technologies, USA) with a piezoscanner of maximum range 9 μm. A micro fabricated silicon cantilever of length 225 μm with a nominal spring force constant of 21–98 N/m was used as nanosensor. Cantilever oscillation frequency was tuned into resonance frequency of 150–300 kHz. The images (512 × 512 pixels) were captured with a scan size between 0.5 and 5 μm. Images were processed by flattening using Pico Scan software (Molecular Imaging Corporation, USA).

For mass spectrometric analysis, samples of peptides were desalted using Zip-Tip μ-C₁₈ column filters (Millipore, Billerica, MA, USA). Matrix-bound peptides were eluted by 50% acetonitrile containing 0.01% trifluoroacetic acid (TFA). The samples were desolvated at 100–125°C and analysed under positive mode of electrospray ionization (ESI) using a Q-ToF Mass Spectrometer (Waters Corporation, USA). Deconvolution of the raw spectra was done with MaxEnt1 algorithm.

Inactive bromelain was prepared after treating the enzyme (1 mg/ml in buffer A) with 5 μM of iodoacetamide for 30 min at 25°C in the dark. Excess reagent was removed by exhaustive dialysis against buffer A. To ensure complete inactivation, modified bromelain was heated at 100°C for 5 min. Turbidity of the solution was removed by centrifugation. Proteolytic activity of this preparation was beyond detection by azocasein assay or zymography.

Proteolysis of bromelain under conditions similar to human digestive system was done as follows: bromelain (100 mg) in 2 ml of 5% formic acid (pH ~2.0) was stirred. The insoluble material was removed by centrifugation. Pepsin (2 mg, 1 : 50 wt/wt) was added to the solution and was incubated at 37°C for 4 h. Thereafter, NH₄HCO₃ was added to increase the pH to 7.5. Trypsin and chymotrypsin (2 mg each, 1 : 50 wt/wt) along with trace amounts of elastase and carboxypeptidase (type-II PMSF-treated) were added for digestion at 37°C for 8 h. This was followed by an additional incubation with BBM proteases for 4 h. These incubation conditions were at par foods that are exposed in the human gastrointestinal tract, as far as possible.

To follow inhibition of aggregate formation, if any, Aβ₄₀ (0.1 mg/ml) was incubated in buffer A containing 100 mM NaCl for 18 h at 37°C in the presence of 5–160 μg/ml of bromelain. Also, bromelain was either proteolytically active or inactive or auto-digested or digested by proteases as par human digestive system. All forms of bromelain were incubated under identical conditions as controls to follow self-aggregation of peptides generated from bromelain itself.

Small peptides formed after proteolysis of bromelain were separated from the undigested enzymes along with large polypeptides after passing through Sephadex G-10 SE-column (71 × 1.2 cm, fractionation range >700 Da). The column was fitted to a Bio-Logic Duo Flow instrument (Bio-Rad laboratories) under 4–6 psi pressure, equilibrated with buffer A at a flow rate of 6 ml/h. Elution of protein/peptides was followed continuously at 220 and 280 nm using Biologic Quad Tec UV-vis detector. Fraction size was 2 ml. Peptide concentration was determined using $\epsilon_{214\text{ nm}} = 923\text{ M}^{-1}\text{ cm}^{-1}$ (ref. 23). Mass of peptides present in each fraction was determined by mass spectrometry. Fractions containing peptides of $M_w < 700$ Da were pooled.

Prediction of peptides from bromelain causing disaggregation of Aβ amyloids was done using bioinformatic tools. The sequence of 212 amino acid residues of bromelain and mass of small peptides generated from MS spectrum as stated above were provided as input in Interactive FindPept Analysis software. The software generated a large number of small peptide sequences corresponding to the observed masses and sequence of bromelain. Comparing the sequence of bromelain with Aβ₄₂ using ClustalW (multiple sequence alignment) software, probable sequences of potent peptides from bromelain interacting with Aβ peptide were predicted (described in detail later in the text). This prediction was based on the assumption that peptides which have strong homology with the sticky region of Aβ peptide (residues 15–22) interact most favourably with the aggregates.

Cytotoxic effect of Aβ aggregates on human neuroblastoma cells (SH-SY5Y) was estimated from MTT assay. Cells were maintained in DMEM/Ham's F-12 (1 : 1 v/v) medium supplemented with 10% FBS, 2 mM L-glutamine, 1% penicillin/streptomycin antibiotics and 0.2% antimycotic agent. Cells were grown at 37°C in 95% air/5% CO₂. Harvested cells were plated in 96-well polystyrene plates (Corning Inc., Corning, NY, USA) with approximately 10,000 cells/100 μl of medium/well. Plates were incubated at 37°C for 24 h to attach the cells. Aβ₄₂ (1 μM) was pre-incubated for 24 h in the presence and absence of bromelain-derived peptides, diluted with fresh medium and added to individual wells. The same volume of medium was added to control cultures. The plates were incubated for an additional period of 48 h at 37°C. Cell viability was determined after addition of 10 μl of 5 mg/ml of MTT to each well²⁴. After incubation for 4 h at 37°C, the medium was aspirated and 100 μl of DMSO was added to each well followed by agitation for 10 min. A multi-well assay plate reader (BioTek-Epoch, BioTek Instruments, Inc.) was used for measurement of A_{595 nm}. Cell viability was calculated by dividing the absorbance of the solutions of the wells containing test samples by the absorbance of wells containing medium alone after background correction for each. All data are expressed as mean ± SD. Significant differences of data were calculated by Student's *t*-test after analysis of variance. Probability

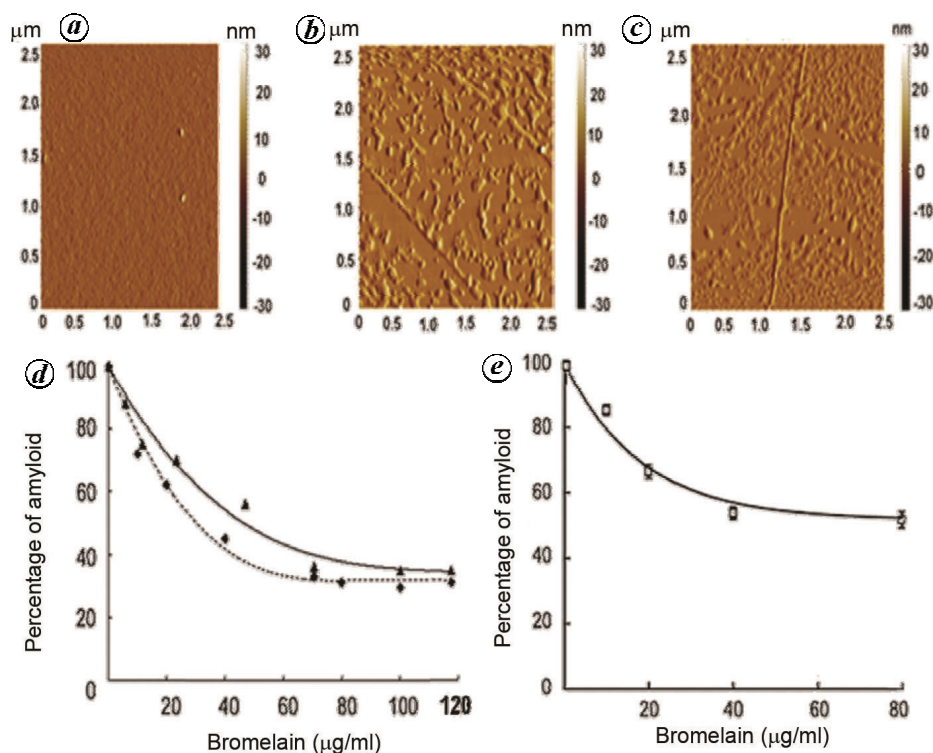


Figure 1. *a–c*, Atomic force microscopy view of various states of A β 40: (*a*) Monomeric state; (*b*) Soluble oligomeric state and (*c*) Prefibrillar state. *d*, *e*, Susceptibility of amyloid aggregates to bromelain. (*d*) Residual amyloid structure (%) of preformed aggregates of A β 40 after digestion with variable concentration of bromelain for 24 h (triangle) and autodigested bromelain for 18 h (diamond). (*e*) Same as that of (*d*) but with inactive bromelain for 24 h. Each point presents an average of three sets where variation was $\pm 10\%$.

values of $P < 0.05$ were considered to represent significant differences.

Formation of oligomeric and proto-fibrillar states of A β 40/42 monitored using AFM. While the monomeric state of A β 40 showed very few small multimers, the oligomeric state was comprised of a good number of molecular associates of variable shape and size (Figure 1 *a* and *b*). The fibrillar state showed formation of long thread-like fibres along with oligomeric products (Figure 1 *c*). This structure also showed intense emission in the ThT assay (shown later). The process of oligomerization was controlled so that the final state remained soluble. These soluble states are more toxic than the insoluble amyloid fibrils and are better targets for controlling amyloid depositions^{25–28}. Disaggregation of A β 40 was quantified by ThT assay after incubation with variable concentrations of bromelain for 18 h. The bromelain was either functionally active or inactive or autodigested. The first two varieties contained intact bromelain. It was observed that all forms of bromelain were capable of destabilizing A β 40 amyloid aggregates. Active and autodigested bromelain at 80 $\mu\text{g/ml}$ disassembled the aggregates by 58–60% (Figure 1 *d*). Interestingly, inactive bromelain also caused destabilization but to a lesser extent of nearly 40% (Figure 1 *e*). These results collectively indicated that the proteolytic activity of bromelain

was not of primary importance in this phenomenon. Rather the surface of the molecule or to be more precise, stretches of amino acid sequences of bromelain caused the disintegration of the amyloid aggregate.

Bromelain was digested with proteases similar to human digestive system to generate small peptides. Under these conditions, autodigestion of bromelain did not dominate. A β 40 aggregates were degraded more efficiently by this pool of peptides as observed from the ThT assay. When incubated for 24 h at 37°C in the presence of 0–155 μM of the peptides, the extent of disaggregation approached near completion (Figure 2 *a*). The time course of disaggregation was followed using as low as 5 μM of the peptides for 72 h, where an exponential rate of reaction was observed (Figure 2 *b*). Under these conditions, nearly 90% of disaggregation was observed. The disaggregation was also verified by microscopic observations. TEM images showed the presence of fibrillar structure of A β 40 aggregate whereas the mesh-like structures were reduced to an agglomeration of oligomeric structures after 24 h of incubation with bromelain peptides (Figure 2 *c*, upper and lower panels). In Figure 2 *c*, the lower panel capture, an event where a large aggregate is being fragmented into smaller components. AFM profile of the destabilized aggregate showed that the rod-like fibrillar structures were reduced to fragmented lumps

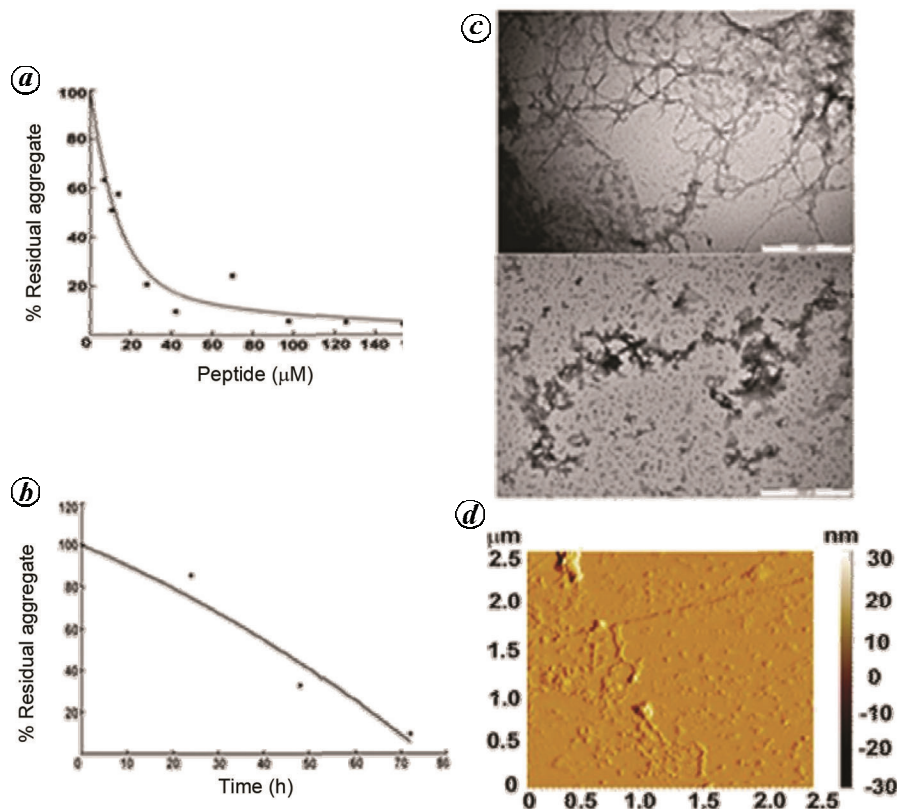


Figure 2. Residual amyloid structure (%) of preformed aggregates of A β 40. *a*, Variable concentration of the pool of peptides obtained from bromelain after protease digestion. *b*, Time course of the same reaction with 28 μ M of peptides. Each point presents an average of three sets where variation was $\pm 10\%$. *c*, TEM images of fibrillar structure of A β 40 (upper panel) and its degraded form after incubation with the pool of peptides (lower panel). A control set using only bromelain peptides did not show self-aggregation detected by transmission electron microscope. *d*, AFM image of the degraded form of fibrillar structures of A β 40.

(Figure 2 *d*). When the period of incubation was continued for 72–96 h, the oligomeric structures gradually disappeared.

When bromelain is hydrolysed by digestive enzymes, one cannot exclude the presence of some undigested proteins and large polypeptides among the products. Since inactive bromelain can destabilize amyloid aggregates and peptides of >700 Da cannot cross the blood brain barrier (BBB), very small peptides were separated from the peptide pool by Sephadex G-10 gel filtration chromatography. From the eluent, four fractions of 1 ml each were collected. These fractions correspond to the positions marked I–IV in Figure 3 *a*. Assuming that the fraction corresponding to void volume contained undigested bromelain and its large fragments, it was not considered. Rest of the collected fractions were rechromatographed under identical conditions (Figure 3 *b*, II–IV). Assuming that the first two partially resolved peaks contain high M_w proteins/peptides, rechromatograms showed greater abundance of small peptides from II to IV. These fractions supposedly contain peptides of very low M_w . The mass distribution of the peak top of the third fractions of

Figure 3 *b* (I–IV) was verified (Figure 3 *c–e*). In all cases, majority of the peptides detected were of $M_w < 700$ Da and thus are supposed to cross BBB as far as M_w is concerned²⁹.

Towards prediction of peptides causing disaggregation, amino acid sequences of bromelain and A β 42 were aligned using ClustalW2 software. Residues 16–22 (KLVFFAE) of A β 42 form amyloid of their own and very likely form the core of the whole molecular fibrils³⁰. This is the most aggregate-prone region of the A β peptide. This region shows strong homology with 168–174 (DSIIYPK) residues of bromelain. A tryptophan-rich sequence of bromelain KKWGAKWG (174–181) also shows significant homology next to the aggregate-prone region of A β 42 (Figure 4, upper panel, marked by bars). Tryptophan being one of the potent amino acids causing aggregation of A β amyloid, this stretch of peptide from bromelain may also interact with the A β conformers³¹. To ascertain the presence of such peptides within the peptide pool, the sequence of bromelain and masses of the digested peptides generated from mass spectrum were supplied as input in the interactive FindPept analysis software. The

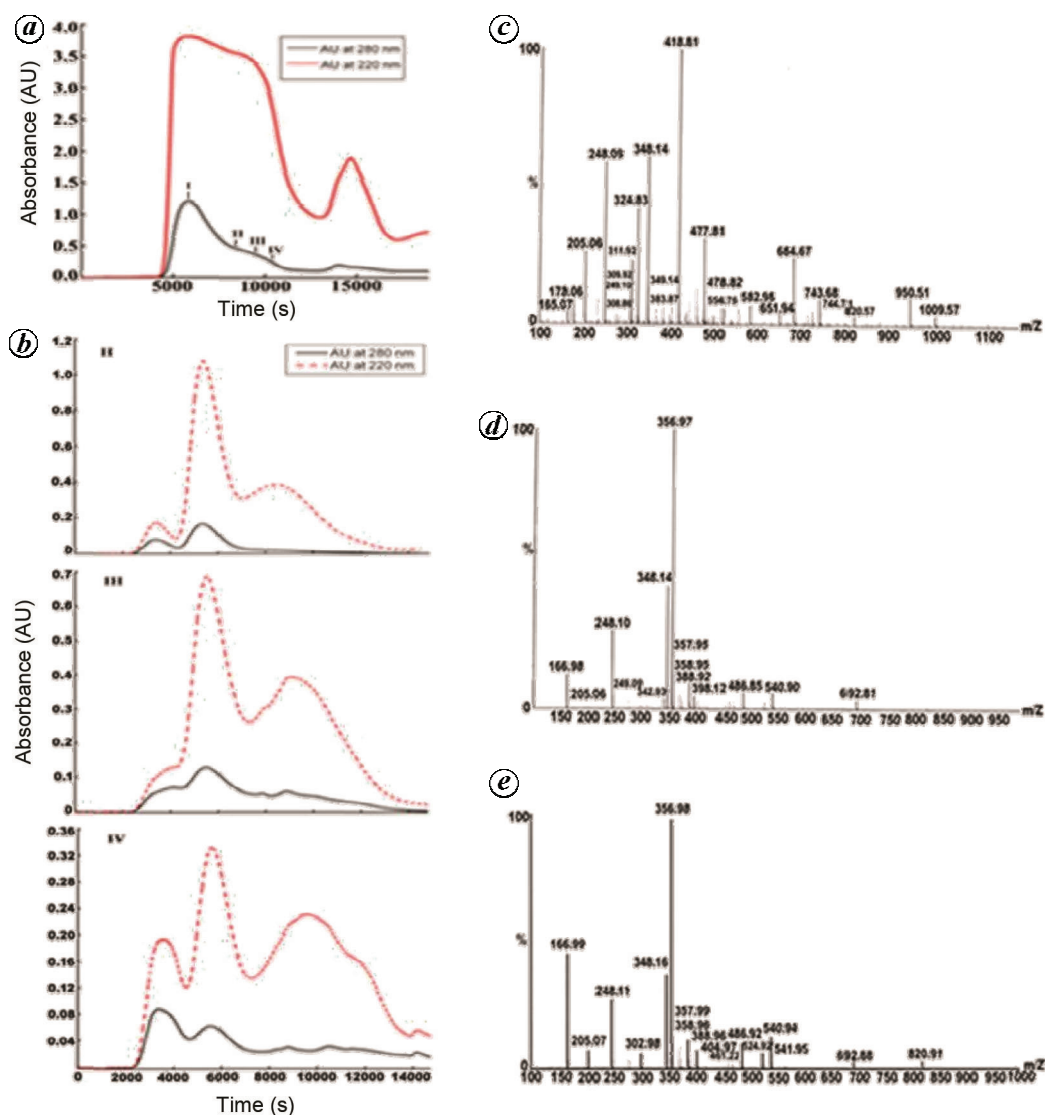


Figure 3. *a*, Separation of peptides generated from bromelain after digestion with proteases by Sephadex G-10 gel filtration chromatography. *b*, II, III and IV are rechromatograms of the fractions marked II, III and IV in (*a*), under identical conditions of gel filtration as in (*a*). In all sets, the upper and lower tracings represent elution profiles followed at 220 and 280 nm respectively. *c–e*, ESI mass spectra of the third peaks of (*b*) (II–IV) monitored at 220 nm.

sequences of peptides generated from mass spectrometric analysis were searched from the sequence of stem bromelain. No peptide stretch within 168–174 residues of bromelain could be detected. Presence of free tryptophan of 205.06 Da from bromelain was observed. However, some tryptophan-rich peptides of identical M_w of 461.25 Da were also detected. These were KWGA (175–178), WGAK (176–179), GAKW (177–180) and AKWG (178–181). Another tryptophan-rich peptide NPCGACWA (21–28, 821.31 Da) was also detected. It was not considered further due to its large size.

Once the peptides causing disaggregation were predicted and their presence in the peptide pool was confirmed from MS data, peptides of sequences KWGA, WGAK, GAKW and AKWG were synthesized. These peptides at

0.01–10.0 μM were incubated with $A\beta_{40}$ aggregates for 15 days and disaggregation was followed by the ThT assay. Among these peptides, GAKW was the most potent where around 60% of disaggregation was achieved (Figure 4 *a*). Other peptides showed disaggregation to variable extents. The effect of the mixture of these synthetic peptides at 1 and 10 μM on disaggregation of $A\beta_{40}$ aggregates was also studied. Over 10 days, disaggregation varied from 50% to 70% (Figure 4 *b*). No synergistic effect of the peptide mixture was observed. Overall, the extent of disaggregation was variable over time, probably because of complications arising from self-aggregation of the synthetic peptides.

Protection of cytotoxicity against 1 μM of $A\beta_{42}$ aggregates on human neuroblastoma cells (SH-SY5Y)

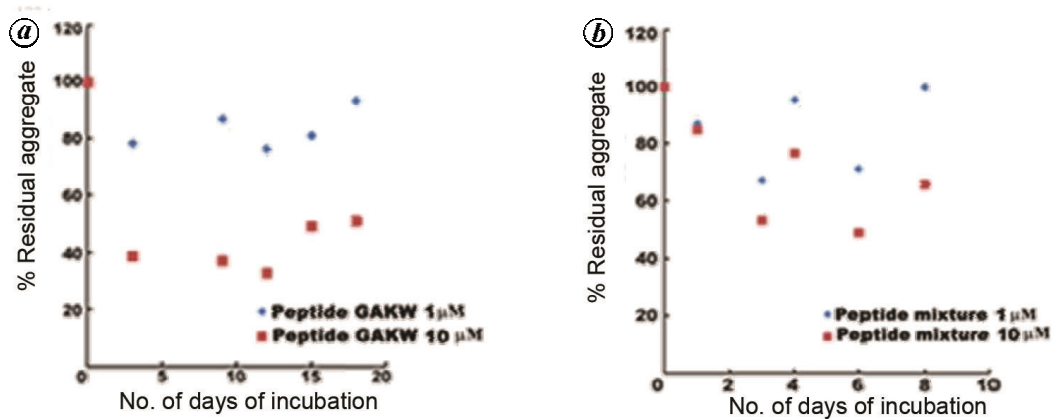
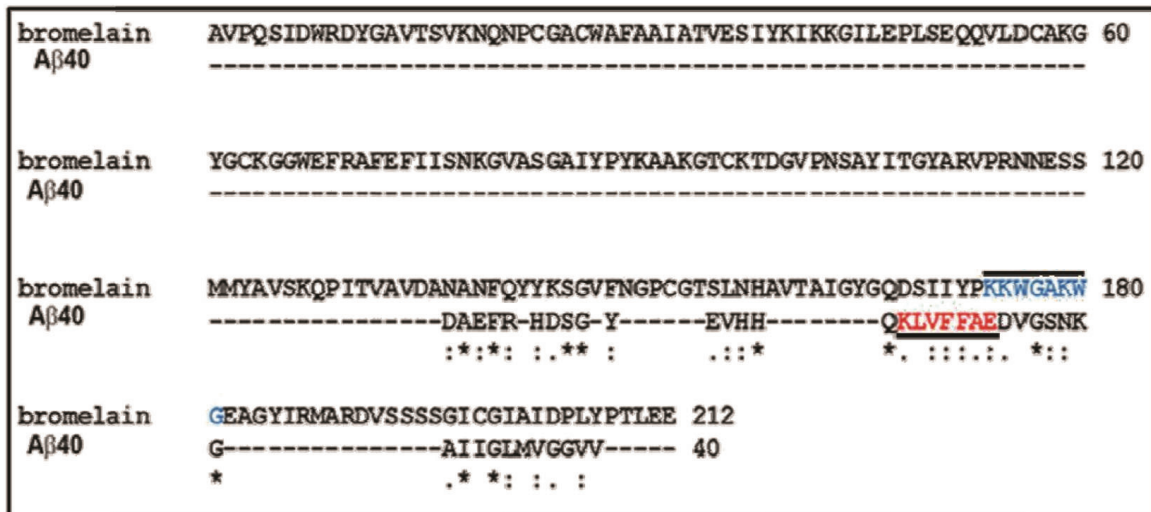


Figure 4. (Upper panel) Sequence alignment of stem bromelain and Aβ peptide (1–40) using ClustalW2 software. (Lower panel) Time course of retention of residual amyloid structure of preformed aggregate of Aβ40 treated with the synthetic peptide GAKW (a) and a pool of other synthetic peptides (b). These results are the average of three sets where variation was ±10%. Disaggregation was followed by thioflavin T assay.

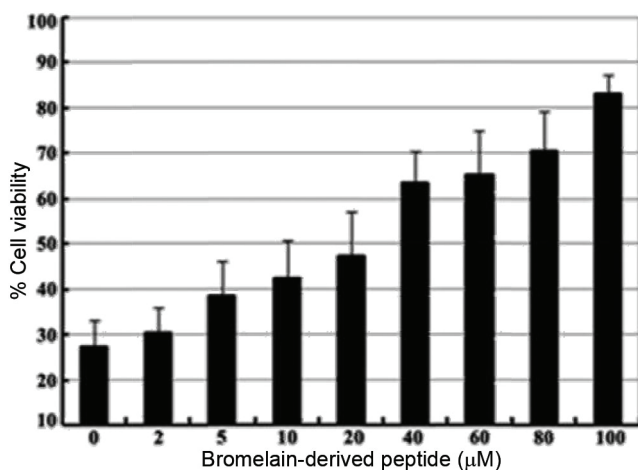


Figure 5. Viability of human neuroblastoma cells (SH-5YSY) grown in the presence of 1 μM of Aβ42 and 0–100 μM of the pool of peptides obtained from protease digestion of bromelain. Average values from five replicate wells were used for each sample and each experiment was repeated thrice. The bar represents variation of results obtained from three sets. Viability was monitored by ThT assay.

by 2–100 μM of bromelain-derived peptides was verified. Results showed that viability of the cells in the presence of toxic aggregates was limited to 28 ± 6%. Cell viability followed direct dependence on the concentration of the peptides, where maximum viability of 82 ± 7% could be achieved. No inconsistency in the results was observed (Figure 5). Morphological patterns of the cells were monitored under phase contrast microscopy. Healthy cells without any treatment were evenly distributed, elongated or oval-shaped, where nuclei and processes were distinctly visible. Morphology of the Aβ oligomer-treated cells was different; the cells were non-uniformly clustered, round-shaped; nuclei were disintegrated and less prominent, and processes were short and indistinct. However, features of the visible cells treated with Aβ oligomer in the presence of bromelain-derived peptides were similar to those of healthy cells. Viability of cells in the presence of PBS or bromelain-derived peptides under identical conditions was similar, indicating that the peptides did not confer toxicity to the cells.

Therefore, we demonstrate that preformed fibrils of A β 40 are destabilized by stem bromelain or peptides derived from this enzyme. This study is confined to soluble pre-fibrillar states of A β , which are the intermediates *en route* formation of β -amyloid plaques. These intermediate structures show higher toxicity to neuronal cells than the fibrils themselves^{25–28}. In this study, initial experiments were performed with A β 40 because it is relatively cheap, aggregate-prone similar to A β 42 and occurs in the blood.

The uptake of any compound in the brain is strictly regulated by the BBB³². The capacity of a peptide to cross the BBB and enter into the brain is dependent upon several compositional factors, including size, flexibility, conformation, sequence and hydrophobic/hydrophilic properties. Among these, molecular weight is a major factor³³. Reviews often quote an absolute cut-off value of 450 Da for penetration into the BBB²⁹. However, during inflammation as in the case of AD, when the integrity of BBB is lost, relatively bigger peptides may cross the barrier depending on the extent of damage. In this study, peptides smaller than 700 Da were separated from the pool of peptides generated from bromelain (Figure 3). These small peptides could effectively destabilize A β aggregates up to 90% as observed from the ThT assay (Figure 2a and b). TEM and AFM images confirmed these findings (Figure 2c and d). Holding the size restriction, probable peptides that are potent for A β disaggregation were identified by ClustalW2 and Interactive FindPept software analysis. Synthetic peptides having these sequences also showed disaggregation of A β 40/42 (Figure 4a and b). Among these peptides, GAKW was the best. In AD, A β 42 peptide deposits as fibrils in neuronal cells of the brain. The peptide pool from bromelain not only destabilized preformed aggregates of A β as observed from *in vitro* experiments, but also prevented growth of the oligomeric states/aggregates that are cytotoxic (Figure 5).

To act efficiently as destabilizing A β aggregates, the peptides from bromelain should qualify the following criteria – the peptides should traverse the BBB, concentration of the peptides around the aggregates should be sufficient to destabilize the latter once administered to patients orally or intravenously, and animal model experiments should give a positive indication. These observations are unknown at present.

Protein aggregation is dynamic in nature, maintaining an equilibration between the oligomeric and monomeric states³⁴. In the presence of antibody against the monomeric molecule, the strong binding between the monomeric state and the corresponding antibody shifts the equilibration towards dissociation of the aggregate³⁵. Several small organic molecules of plant origin like curcumin³⁶, resvitrol³⁷, alpha-tocopherol³⁸, caffeine³⁹, etc. have different degrees of protection against fibril formation. Our recent observation indicates that peptides derived from fruit

bromelain can efficiently dissociate preformed aggregates and also inhibit formation of aggregates from monomeric state of human insulin. It is proposed that binding of the peptides with monomeric insulin once dissociated from the aggregates causes irreversible conformational change, making them incapable of re-aggregation⁴⁰. Dramatic improvement in cell viability as demonstrated in Figure 5 is suggestive of this hypothesis. The hypothesis is supported by the fact that synthetic peptides having the template of a toxin component of Russell's viper venom showed efficient disaggregation of A β amyloid⁴¹. A clearer mechanism of these processes is likely to be unveiled in near future.

1. Kopito, R. R., Aggresomes, inclusion bodies and protein aggregation. *Trends Cell Biol.*, 2000, **10**, 524–530.
2. Tiraboschi, P., Hansen, L. A., Thal, L. J. and Corey-Bloom, J., The importance of neuritic plaques and tangles to the development and evolution of AD. *Neurology*, 2004, **62**, 1984–1989.
3. Mathis, C. A., Lopresti, B. J. and Klunk, W. E., Impact of amyloid imaging on drug development in Alzheimer's disease. *Nucl. Med. Biol.*, 2007, **34**, 809–822.
4. Kelly, G. S., Bromelain: a literature review and discussion of its therapeutic applications. *Altern. Med. Rev.*, 1996, **1**, 243–257.
5. Rowan, A. D., Buttle, D. J. and Barrett, A. J., The cysteine proteinases of the pineapple plant. *Biochem. J.*, 1990, **266**, 869–875.
6. Kumakura, S., Yamashita, M. and Tsurufuji, S., Effect of bromelain on kaoline-induced inflammation in rats. *Eur. J. Pharmacol.*, 1988, **150**, 295–301.
7. Maurer, H. R., Bromelain: biochemistry, pharmacology and medical use. *Cell. Mol. Life Sci.*, 2001, **58**, 1234–1245.
8. Pirotta, F. and de Giuli-Morghen, C., Bromelain: anti-inflammatory and serum fibronolytic activity after oral administration in the rat. *Drugs Exp. Clin. Res.*, 1978, **4**, 1–20.
9. Das, S. and Bhattacharyya, D., Bromelain from pineapple: its stability and therapeutic potential. In *Tropical Fruits: from Cultivation to Consumption and Health Benefits, Pineapple* (eds Bogson, C. S. and Todorov, S. D.), Nova Science Publishers, Hauppauge, NY, USA, 2017, pp. 43–100.
10. Dutta, S. and Bhattacharyya, D., Enzymatic, antimicrobial and toxicity studies of the aqueous extract of *Ananus comosus* (pineapple) crown leaf. *J. Ethnopharmacol.*, 2013, **150**, 451–457.
11. Kim, M. J., Chae, S. S., Koh, Y. H., Lee, S. K. and Jo, S. A., Glutamate carboxypeptidase II: an amyloid peptide-degrading enzyme with physiological function in the brain. *FASEB J.*, 2010, **24**, 4491–4502.
12. Wolfe, M. S., γ -Secretase inhibitors and modulators for Alzheimer's disease. *J. Neurochem.*, 2012, **120**, 89–98.
13. Badman, M. K., Pryce, R. A., Charge, S. B., Morris, F. and Clark, A., Fibrillar islet amyloid polypeptide (amylin) is internalized by macrophages but resists proteolytic degradation. *Cell Tissue Res.*, 1998, **291**, 285–294.
14. Mueller-Stieber, S. *et al.*, Anti-amyloidogenic and neuroprotective functions of cathepsin B: implications for Alzheimer's disease. *Neuron*, 2006, **51**, 703–714.
15. Sun, B. *et al.*, Cystatin C-cathepsin B axis regulates amyloid beta levels and associated neuronal deficits in an animal model of Alzheimer's disease. *J. Neurosci.*, 2008, **28**, 247–257.
16. De Strooper, B., Proteases and proteolysis in Alzheimer disease: a multifactorial view on the disease process. *Physiol. Rev.*, 2010, **90**, 465–494.
17. Hasanbasic, S., Jahic, A., Karahmet, E., Sejranic, A. and Prnjavorac, B., The role of cysteine proteases in Alzheimer disease. *Mater. Sociomed.*, 2016, **28**, 235–238.

18. Mukherjee, D., Multimeric proteins: its adaptation and regulation of biological activities. Ph.D thesis, Jadavpur University, Kolkata, India, 2012.
19. Cheeseman, C. I. and O'Neill, D., Isolation of intestinal brush-border membranes. *Curr. Protoc. Cell Biol.*, 2006, **30**, 3.21.1–3.21.10.
20. Bhattacharya, R., Fruit and stem bromelain from pineapple (*Ananas comosus*): stabilization and biochemical characterization of the enzymes. Ph.D thesis, Jadavpur University, Kolkata, India, 2009.
21. Sarath, G., Motte, R. S. D. L. and Wagner, F. W., Protease assay methods. In *Proteolytic Enzymes: A Practical Approach* (eds Beynon, R. J. and Bond, J. S.), IRL Press, Oxford University Press, Oxford, UK, 1996, pp. 25–55.
22. Soto, C., Sigurdsson, E. M., Morelli, L., Kumar, R. A., Castano, E. M. and Frangione, B., β -Sheet breaker peptides inhibit fibrillogenesis in a rat brain model of amyloidosis: implications for Alzheimer's therapy. *Nature Med.*, 1998, **4**, 822–826.
23. Kuipers, B. J. H. and Gruppen, H., Prediction of molar extinction coefficients of proteins and peptides using UV absorption of the constituent amino acids at 214 nm to enable quantitative reverse phase high-performance liquid chromatography–mass spectrometry analysis. *J. Agric. Food Chem.*, 2007, **55**, 5445–5451.
24. Shearman, M. S., Hawtin, S. R. and Tailor, V. J., The intracellular component of cellular 3-(4,5-dimethylthiazol-2-yl)-2,5-diphenyltetrazolium bromide (MTT) reduction is specifically inhibited by β -amyloid peptides. *J. Neurochem.*, 1995, **65**, 218–227.
25. Caughey, B. and Lansbury, P. T., Protofibrils, pores, fibrils, and neurodegeneration: separating the responsible protein aggregates from the innocent bystanders. *Annu. Rev. Neurosci.*, 2003, **26**, 267–298.
26. Chimon, S., Shaibat, M. A., Jones, C. R., Calero, D. C., Aizezi, B. and Ishii, Y., Evidence of fibril-like β -sheet structures in a neurotoxic amyloid intermediate of Alzheimer's β -amyloid. *Nature Struct. Mol. Biol.*, 2007, **14**, 1157–1164.
27. Hoshi, M., Sato, M., Matsumoto, S., Noguchi, A., Yasutake, K., Yoshida, N. and Sato, K., Spherical aggregates of β -amyloid (amylospheroid) show high neurotoxicity and activate tau protein kinase I/glycogen synthase kinase-3 β . *Proc. Natl. Acad. Sci. USA*, 2003, **100**, 6370–6375.
28. Lambert, M. P. *et al.*, Diffusible, nonfibrillar ligands derived from $A\beta_{1-42}$ are potent central nervous system neurotoxins. *Proc. Natl. Acad. Sci. USA*, 1998, **95**, 6448–6453.
29. Banks, W. A., Characteristics of compounds that cross the blood–brain barrier. *BMC Neurol.*, 2009, **9**, S1–S3.
30. Hamley, I. W., Peptide fibrillization. *Angew Chem. Int. Ed.*, 2007, **46**, 8128–8147.
31. Attali, R. S. *et al.*, Complete phenotypic recovery of an Alzheimer's disease model by a quinine–tryptophan hybrid aggregation inhibitor. *PLoS ONE*, 2010, **5**, 1–15.
32. Crone, C., The blood–brain barrier – facts and questions. In *Ion Homeostasis of the Brain* (eds Siesjo, B. and Sorensen, S.), Munksgaard, Copenhagen, Denmark, 1971, pp. 52–62.
33. Witt, K. A. and Davis, T. P., CNS drug delivery: opioid peptides and the blood–brain barrier. *AAPS J.*, 2006, E76–88; <http://www.aapsj.org>
34. Kim, S., Nollen, E. A., Kitagawa, K., Bindokas, V. P. and Morimoto, R. I., Polyglutamine protein aggregates are dynamic. *Nature Cell Biol.*, 2002, **4**, 826–831.
35. Lecerf, J. M. *et al.*, Human single-chain Fv intrabodies counteract *in situ* Huntington aggregation in cellular models of Huntington's disease. *Proc. Natl. Acad. Sci. USA*, 2001, **98**, 4764–4769.
36. Yang, F. *et al.*, Curcumin inhibits formation of amyloid beta oligomers and fibrils, binds plaques, and reduces amyloid *in vivo*. *J. Biol. Chem.*, 2005, **280**, 5892–5901.
37. Karuppagounder, S. S., Pinto, T., Xu, H., Chen, H. L., Beal, M. F. and Gibson, G. E., Dietary supplementation with resveratrol reduces plaque pathology in a transgenic model of Alzheimer's disease. *Neurochem. Int.*, 2009, **54**, 111–118.
38. Yamada, K., Tanaka, T., Han, D., Senzaki, K., Kameyama, T. and Nabeshima, T., Protective effects of idebenone and alpha-tocopherol on beta-amyloid-(1-42)-induced learning and memory deficits in rats: implication of oxidative stress in beta-amyloid-induced neurotoxicity *in vivo*. *Eur. J. Neurosci.*, 1999, **11**, 83–90.
39. Cao, C. *et al.*, Caffeine suppresses amyloid- β levels in plasma and brain of Alzheimer's disease transgenic mice. *J. Alzheimers Dis.*, 2009, **17**, 681–697.
40. Das, S. and Bhattacharyya, D., Destabilization of human insulin fibrils by peptides of bromelain derived from *Ananas comosus* (pineapple). *J. Cell. Biochem.*, 2017, **118**, 4881–4896.
41. Bhattacharjee, P. and Bhattacharyya, D., Factor V activator from *Daboia russelli russelli* venom destabilizes β -amyloid aggregate, the hallmark of Alzheimer disease. *J. Biol. Chem.*, 2013, **288**, 30559–30570.

ACKNOWLEDGEMENTS. The research was supported by Cognition Science Initiative programme of DST, New Delhi awarded to D.B. (SR/CSI/07/2009). D.B. was also partly supported by DBT-Visiting Research Fellowship for development of North-East India. D.M., P.B. and R.B. were supported by fellowships from DST, UGC-NET and CSIR-SRF, New Delhi respectively. We thank Namrata Singh, CSIR-IICB for help with the figures and Prof. Subrata Pal (Department of Life Sciences and Biotechnology, Jadavpur University, Kolkata) for providing cell culture facility.

Received 15 December 2017; revised accepted 3 August 2018

doi: 10.18520/cs/v115/i11/2133-2141

Performance analysis of South-Indian mushroom units: imperative policy implications for their preparedness for global competitiveness

Mahantesh Shirur^{1,*}, N. S. Shivalingegowda², M. J. Chandregowda³ and Rajesh K. Rana⁴

¹ICAR-Directorate of Mushroom Research, Solan 173 213, India

²Department of Agricultural Extension, UAS, GKVK, Bengaluru 560 065, India

³ICAR-Agricultural Technology Application Research Institute, Zone-VII, Hebbal, Bengaluru 560 024, India

⁴ICAR-National Institute of Agricultural Economics and Policy Research, DPS Marg, Pusa, New Delhi 110 012, India

A highly specialized six-dimensional performance index was designed to comprehensively analyse complex mushroom enterprises having components and estimates, viz. scale/size of the enterprise (4.225), infrastructure/machinery employed (4.539), social capital indicators (4.696), efficiency indicators (6.346), good mushroom cultivation practices (5.246) and incremental expansion (3.597). Sixty edible mushroom growing enterprises of Karnataka were selected for

*For correspondence. (e-mail: mshirur.icar@gov.in)